

Radiation exposure and establishment of diagnostic reference levels of whole-body low-dose CT for the assessment of multiple myeloma with second- and third-generation dual-source CT

Acta Radiologica
2022, Vol. 63(4) 527–535
© The Foundation Acta Radiologica
2021
Article reuse guidelines:
sagepub.com/journals-permissions
DOI: 10.1177/02841851211003287
journals.sagepub.com/home/acr


Sebastian Zensen¹ , Denise Bos¹ , Marcel Opitz¹ ,
Johannes Haubold¹ , Michael Forsting¹, Nika Guberina² and
Axel Wetter¹

Abstract

Background: In the assessment of diseases causing skeletal lesions such as multiple myeloma (MM), whole-body low-dose computed tomography (WBLDCT) is a sensitive diagnostic imaging modality, which has the potential to replace the conventional radiographic survey.

Purpose: To optimize radiation protection and examine radiation exposure, and effective and organ doses of WBLDCT using different modern dual-source CT (DSCT) devices, and to establish local diagnostic reference levels (DRL).

Material and Methods: In this retrospective study, 281 WBLDCT scans of 232 patients performed between January 2017 and April 2020 either on a second- (A) or third-generation (B) DSCT device could be included. Radiation exposure indices and organ and effective doses were calculated using a commercially available automated dose-tracking software based on Monte-Carlo simulation techniques.

Results: The radiation exposure indices and effective doses were distributed as follows (median, interquartile range): (A) second-generation DSCT: volume-weighted CT dose index ($CTDI_{vol}$) 1.78 mGy (1.47–2.17 mGy); dose length product (DLP) 282.8 mGy·cm (224.6–319.4 mGy·cm), effective dose (ED) 1.87 mSv (1.61–2.17 mSv) and (B) third-generation DSCT: $CTDI_{vol}$ 0.56 mGy (0.47–0.67 mGy), DLP 92.0 mGy·cm (73.7–107.6 mGy·cm), ED 0.61 mSv (0.52–0.69 mSv). Radiation exposure indices and effective and organ doses were significantly lower with third-generation DSCT ($P < 0.001$). Local DRLs could be set for $CTDI_{vol}$ at 0.75 mGy and DLP at 120 mGy·cm.

Conclusion: Third-generation DSCT requires significantly lower radiation dose for WBLDCT than second-generation DSCT and has an effective dose below reported doses for radiographic skeletal surveys. To ensure radiation protection, DRLs regarding WBLDCT are required, where our locally determined values may help as benchmarks.

Keywords

Radiation exposure, multiple myeloma, computed tomography, whole body imaging, radiation dosimetry

Date received: 3 January 2021; accepted: 24 February 2021

Introduction

Multiple myeloma (MM) is a hematological malignancy characterized by usually multicentric abnormal proliferation of monoclonal plasma cells showing variable degrees of differentiation (1). Progressive bone marrow infiltration with replacement of myelopoiesis leads to typical bone destruction including osteolysis, osteopenia, and seldomly osteosclerosis (2). Diagnosis relies on

¹Department of Diagnostic and Interventional Radiology and Neuroradiology, University Hospital Essen, Essen, Germany

²Department of Radiotherapy, University Hospital Essen, Essen, Germany

Corresponding author:

Sebastian Zensen, Department of Diagnostic and Interventional Radiology and Neuroradiology, University Hospital Essen, Hufelandstraße 55, 45147 Essen, Germany.
Email: sebastian.zensen@uk-essen.de

bone marrow histology and one of the following clinical features: hypercalcemia; renal insufficiency; anemia; and bone lesions (3). Furthermore, evidence of lytic bone lesions defines active disease, for which immediate treatment is required (3). Novel therapies have improved the survival of MM within recent decades (4). Therefore, a sensitive imaging modality is crucial for the diagnosis and surveillance of MM (5). In the past, the imaging work-up for MM was a survey including about 20 conventional radiographs (6). While bone lesions in the appendicular skeleton are well recognized by both conventional radiography and computed tomography (CT), lesions in the spine, thoracic cage, and skull are substantially better displayed by CT (7).

As the detection of bone lesions by conventional radiography is limited, various cross-sectional imaging modalities such as whole-body low-dose CT (WBLDCT), magnetic resonance imaging (MRI), and hybrid imaging such as positron emission tomography (PET)/CT have been shown to be more sensitive and provide additional diagnostic information (7,8). Hence, by improving diagnosis and surveillance, WBLDCT optimizes treatment of MM. In addition, the European Myeloma Network suggested a preference for WBLDCT as the standard imaging modality for the assessment of bone lesions in MM (5). Besides, WBLDCT is suitable for the assessment of other diseases that cause multiple skeletal lesions such as fibrous dysplasia, eosinophilic granuloma, enchondroma, hyperparathyroidism, or infections. Alongside these benefits, CT has been considered a high-dose imaging technique since its establishment, and causes the major part of collective effective dose for all radiographic examinations and has even increased within the last few years (9,10). While some recent studies reported radiation doses of WBLDCT for MM, further detailed dose assessment and comparison between modern CT generations is needed to optimize radiation protection. Additionally, specific reports of effective and organ doses as well as diagnostic reference levels (DRLs) of new generation CT scanners are rare. Furthermore, because several patients with MM undergo WBLDCT repeatedly, dose protection is indispensable. For various indications, DRLs were established to limit radiation exposure of radiological imaging modalities (11). Nonetheless, neither European nor national DRLs are set up for WBLDCT and published local DRLs are rare. To compare and evaluate local radiation exposure distributions and optimize radiation protection, 75th percentiles of dose metric distributions are often used as DRLs (12).

The aim of the present study was to evaluate the radiation exposure and dose assessment and to establish local DRLs of WBLDCT at modern second- and third-generation dual-source CT (DSCT) devices for

the assessment of diseases causing skeletal lesions such as MM.

Material and Methods

Patient cohort

Ethical approval for this retrospective single-center study was granted by the institutional review board and the requirement to obtain informed consent was waived (20-9321-BO). Patients clinically referred for a WBLDCT for the assessment of MM on a second- or third-generation DSCT between January 2017 and April 2020 were identified using a Digital Imaging and Communications in Medicine (DICOM) header based tracking and monitoring software (Radimetrics Enterprise Platform, Bayer Healthcare, Leverkusen, Germany).

Dual-source CT devices and whole-body low-dose CT protocols

Patients were examined on one of two commercially available multislice DSCT scanners: second-generation dual-source 128-slice SOMATOM Definition Flash and third-generation dual-source 192-slice SOMATOM Force (both Siemens Healthineers, Forchheim, Germany). With the SOMATOM Definition Flash, patients were scanned with the following parameters: 100 kV; collimation = 128×0.6 mm; gantry rotation time = 0.5 s; and reference tube current-time product = 70 mAs. At SOMATOM Force patients were scanned with these parameters: 100 kV with additional spectral shaping by a tin filter (Sn); collimation = 192×0.6 mm; gantry rotation time = 0.5 s; and reference tube current-time product = 130 mAs. With both devices, only tube A was used for image acquisition and automated tube current modulation (Care Dose 4D, Siemens Healthineers, Germany) was applied. Image reconstruction techniques were applied to both DSCT with a moderate strength of 3 (levels 1–5, where a higher number implies a stronger noise reduction): on SOMATOM Definition Flash Sinogram Affirmed Iterative Reconstruction (SAFIRE, Siemens Healthineers) and on SOMATOM Force Advanced Modeled Iterative Reconstruction (ADMIRE, Siemens Healthineers). Technical settings according to device are summarized in Table 1. All patients were scanned without administration of contrast medium, in the craniocaudal direction, positioned supine, with their head first, and arms alongside the body. All scans were acquired in inspiratory breath-hold during the scanning through the thorax and the upper abdomen.

Table 1. Technical parameters of whole-body low-dose CT for the assessment of multiple myeloma at second- and third-generation DSCT.

CT device	Siemens SOMATOM Definition Flash	Siemens SOMATOM Force
Type	Second-generation DSCT	Third-generation DSCT
Dual-source mode	Off	Off
No. of examinations	118	163
Slices per rotation	128	192
Tube voltage (kVp)	100	100*
Collimation (mm)	128 × 0.6	192 × 0.6
Detector width (mm)	52.5	38.4
Reference tube current-time product (mAs)	70	130
Automated tube current modulation	On	On
Rotation time (s)	0.5	0.5
Pitch	0.6	0.9

*With spectral shaping by tin (Sn) filtration.

CT, computed tomography; DSCT, dual-source computed tomography.

Dose assessment

All examination parameters were retrieved from the control system and radiation exposure measurements referred to the 32-cm diameter standard polymethyl methacrylate (PMMA) CT dosimetry phantom. For dose assessment, the commercially available automated dose-tracking software Radimetrics Enterprise Platform (Bayer Healthcare, Leverkusen, Germany) based on Monte-Carlo simulation techniques was used. All examination data and dose assessments were extracted from this software, which collects radiation exposure metadata and patient demographic information from the DICOM header and from the Radiation Dose Structured Report, which is stored in the Picture Archiving and Communication System (PACS) (13). Assessed radiation exposure indices were the volume-weighted CT dose index ($CTDI_{vol}$) and the dose length product (DLP), which are appropriate parameters to enable radiation protection. Although they do not directly represent the dose to an individual patient, $CTDI_{vol}$ and DLP quantify the radiation dose output of a CT scanner and might help to ensure lower radiation exposures. In addition to that, the effective dose takes the radiosensitivity of organs into account and can be calculated out of the DLP by using specific weighting factors (14). For the present study, the dose-tracking software applied weighting factors following the International Commission on Radiological Protection (ICRP) 103 published in 2007 (15). The following organ doses were determined: adrenal glands; brain; colon; esophagus; eye lenses; gall bladder; heart; kidneys; liver; lungs; muscle; pancreas; red bone marrow; salivary glands; skeleton; skin; small intestine; spleen; stomach; thyroid; thymus; and urinary bladder. Regarding the reproductive system, organ doses of the breasts, ovaries, and uterus were calculated in female patients and of the

testicles in male patients. The effective doses for radiographic skeletal surveys were estimated from published data via a literature search using PubMed.

Statistics and data analysis

Statistical analysis was performed using GraphPad Prism 5.01 (GraphPad Software, San Diego, CA, USA). Samples were tested for normal distribution using the Kolmogorov–Smirnov test, Shapiro–Wilk test, and D’Agostino–Pearson test. Normally distributed data are reported as mean ± standard deviation (SD), non-normally distributed data are reported as median and interquartile range (IQR). The Mann–Whitney U test was applied to compare radiation indices and effective and organ doses. *P* values less than 0.05 were considered statistically significant.

Results

Patient cohort

In our retrospective study, 232 patients (mean age = 63.8 ± 12.1 years) who underwent WBLDCT for the screening or surveillance of MM between January 2017 and April 2020 could be included for evaluation, comprising 40.5% (94 out of 232) women. A total of 39 patients underwent recurring WBLDCT (2x: $n=30$, 3x: $n=8$, 4x: $n=1$). A total of 281 WBLDCT scans were performed.

Radiation exposure and DRL

Total radiation exposure was distributed as follows (median, interquartile range [IQR]): $CTDI_{vol} = 0.75$ mGy (0.52–1.68 mGy) and $DLP = 120.0$ mGy·cm (87.5–270.1 mGy·cm). Of all scans, 42% (118 of 281) were performed at second-generation and 58% (163 of

317) at third-generation DSCT. Differentiated by scanner radiation distribution could be depicted as follows (median, IQR): for second-generation DSCT: $CTDI_{vol} = 1.78$ mGy (1.47–2.17 mGy) and $DLP = 282.8$ mGy·cm (224.6–319.4 mGy·cm); and for third-generation DSCT: $CTDI_{vol} = 0.56$ mGy (0.47–0.67 mGy) and $DLP = 92.0$ mGy·cm (73.7–107.6 mGy·cm) (Table 2). Statistical analysis showed significant differences of both $CTDI_{vol}$ and DLP between second- and third-generation DSCT ($P < 0.001$) (Fig. 1). DRL at our institution of WBLDCT for MM could be depicted as follows: $CTDI_{vol} = 0.75$ mGy and $DLP = 120$ mGy·cm.

Effective and organ doses

Total median effective dose was 0.77 mSv (IQR = 0.58–1.81 mSv). Comparing second- and third-generation DSCT, the median effective dose for second-generation DSCT was 1.87 mSv (IQR = 1.61–2.17 mSv) and for third-generation DSCT 0.61 mSv (IQR = 0.52–0.69 mSv) (Table 2). The Mann–Whitney U test revealed significant difference for effective dose between second- and third-generation DSCT, which was about 67% lower with third-generation DSCT ($P < 0.001$) (Fig. 1). Specific organ doses according to DSCT device are shown in Table 3. Likewise, statistical analysis showed significant differences for calculated organ doses between DSCT generations, which were 66.4%–72.2% lower with third-generation DSCT ($P < 0.001$). For both CT scanners, the lowest organ dose was determined for the esophagus (both scanners: median = 0.55 mSv [IQR = 0.43–1.30 mSv]) and the highest for the skeleton (both scanners: median = 2.19 mSv [IQR = 1.61–5.68 mSv]) (Table 3). The highest organ dose reduction was determined for the skeleton where the median organ dose was about 72% lower with third-generation DSCT (1.67 mSv [IQR = 1.42–1.98 mSv] vs 6.01 mSv [IQR = 5.14–6.86 mSv]) ($P < 0.001$). The lowest organ dose reduction was calculated for the adrenal glands, which was

still about 66% lower with third-generation DSCT ($P < 0.001$).

Radiation dose of WBLDCT versus radiographic skeletal survey

At our institution, WBLDCT nearly replaced the conventional radiographic survey. Therefore, in order to compare our results with radiographic radiation exposure, the literature was analyzed systematically for studies that assessed the radiation doses of typical radiographical skeletal surveys for the assessment of MM. Several studies reported effective doses in the range of 0.9–2.5 mSv for skeletal surveys consisting of 11–22 projections (6,16–18). In contrast, WBLDCT using third-generation DSCT required a median effective dose of 0.61 mSv (IQR = 0.52–0.69 mSv). Hence, WBLDCT can be performed with lower effective doses than typical radiographical skeletal surveys.

Discussion

Comparison of second- and third-generation DSCT scanners showed significantly lower radiation exposure, and effective and organ doses for third-generation DSCT. Hence, further dose reduction in WBLDCT is achievable using new generation DSCT scanners where our locally determined DRLs may help as benchmarks.

As the detection of bone lesions by conventional radiography is limited, all advanced imaging modalities aim to better depict the extent of skeletal lesions, bone marrow infiltration, and soft tissue disease. Recently published criteria for the diagnosis of MM include the image-based evidence of lytic bone lesions by CT or MRI (3). While CT and MRI perform equally regarding detection rate, specificity, and sensitivity, MRI is deemed superior over WBLDCT in cases without osteolytic lesions and can monitor treatment response (19–21). Nonetheless, WBLDCT better depicts lesions at risk for fracture than MRI and

Table 2. $CTDI_{vol}$, DLP, and effective dose for whole-body low-dose CT at second- and third-generation DSCT.

	Total (n = 281)	Second-generation DSCT (n = 118, 42%) Siemens SOMATOM Definition Flash	Third-generation DSCT (n = 163, 58%) Siemens SOMATOM Force
$CTDI_{vol}$ (mGy)	0.75 (0.52–1.68)	1.78 (1.47–2.17)	0.56 (0.47–0.67)
DLP (mGy·cm)	120.0 (87.5–270.1)	282.8 (224.6–319.4)	92.0 (73.7–107.6)
Effective dose* (mSv)	0.77 (0.58–1.81)	1.87 (1.61–2.17)	0.61 (0.52–0.69)

Values are given as median (interquartile range).

*Estimated effective dose calculated from DLP following the weighting factors from the International Commission on Radiological Protection (ICRP) 103 (15).

$CTDI_{vol}$, volume-weighted CT dose index; DLP, dose length product; DSCT, dual-source computed tomography.

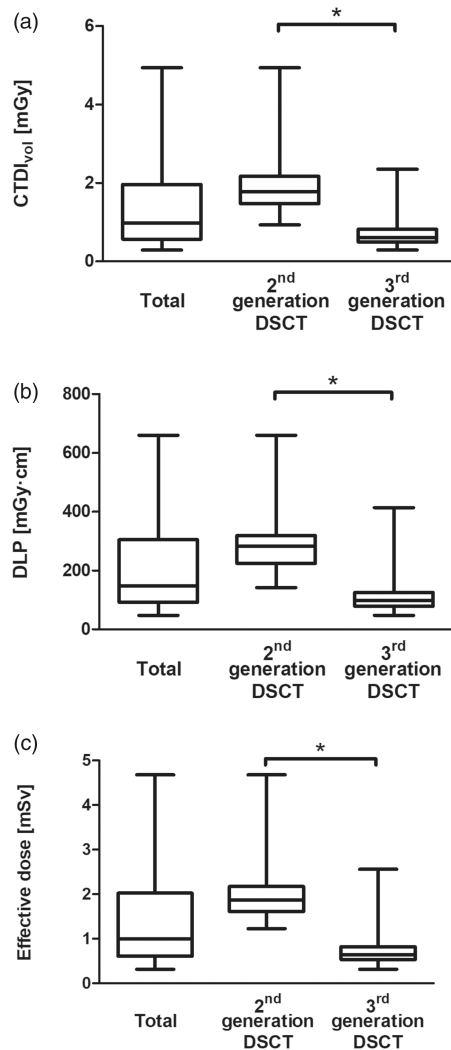


Fig. 1. Distribution of radiation exposure and effective dose of whole-body low-dose CT for the assessment of multiple myeloma. Radiation exposure in terms of (a) CTDI_{vol}, (b) DLP, and (c) effective dose of two modern DSCT devices: second generation DSCT SOMATOM Definition Flash ($n = 118$) and third generation DSCT SOMATOM Force ($n = 163$) (both: Siemens Healthineers, Forchheim, Germany). Estimated effective dose were calculated from DLP following the weighting factors from the International Commission on Radiological Protection (ICRP) 103 (15). Whiskers represent minimum to maximum. Asterisk indicates significant difference ($p < 0.05$). CTDI_{vol}, volume-weighted CT dose index; DLP, dose length product; DSCT, dual-source computed tomography.

lesions <5 mm (2,8). Dual-energy CT plays a specific role for the assessment of MM as it provides additional information about non-osteolytic bone marrow infiltration and may serve as an alternative for patients with contraindications for MRI or FDG-PET/CT (19). While WBLDCT is already used routinely in many institutions, patients would benefit from the expanded diagnostic spectrum, which must not be

limited to lytic bone lesions but also enables evaluation of bone marrow infiltration with precision comparable to MRI and thereby helps to evaluate risk of disease progression (22,23). Considering hybrid imaging modalities, FDG-PET/CT has advantages especially during follow-up, because it can depict active lesions and modified tracer uptake during treatment and thereby predicts outcome (21). Despite the different benefits of all modern imaging modalities, institutional availability of technical equipment affects not least the primary imaging work-up for the assessment of MM. Therefore, CT is the preferred modality because it is widely available and the most sensitive cross-sectional imaging modality in the depiction of bone lesions (7,8). Furthermore, superiority in estimation of fracture risk, shortened examination duration, and possible detection of extraskelatal manifestations are the benefits of WBLDCT compared with a radiographic skeletal survey and outweigh the higher radiation exposure (24). However, potential overexposure to radiation and increased risk of radiation-induced cancer are ongoing concerns to whole-body standard-dose CT, which can result in relatively high effective doses (2,25,26). However, using low-dose techniques for WBLDCT has been shown to provide diagnostic image quality and significantly reduce radiation doses. For example, spectral shaping using tin filters in third-generation DSCT decreases radiation exposure of WBLDCT (27). Additionally, WBLDCT is very accurate for the detection of bone lesions and radiation dose is two- to threefold lower than whole-body standard-dose CT (28,29). In our institution, single-source mode was applied routinely for WBLDCT as it is suitable for the detection of bone lesions. Thus, dual-source mode can be useful for further examination of skeletal lesions such as bone marrow infiltration, where it provides precision comparable with that of MRI (19).

Considering CT radiation doses is indispensable for radiation protection and plays a key role in any optimization process. Several studies assessed radiation exposures of WBLDCT for patients with MM and reported a CTDI_{vol} of 2.89–6.05 mGy and a DLP of 289–784 mGy·cm (6,17,18). Therefore, the radiation exposure in the present study was well below the reported data. Lower radiation exposure could be achieved by modified technical settings such as increased pitch which is inversely proportional to CTDI_{vol}. Furthermore, for the third-generation DSCT scanner, spectral shaping and an advanced iterative reconstruction technique were applied, which have the potential to further reduce radiation exposure. Reported effective doses of WBLDCT are in the range of 1.5–11.3 mSv (6,7,17,27,30). Recently published studies reported effective doses of a typical

Table 3. Comparison of organ doses (mSv) of whole-body low-dose CT at second- and third-generation DSCT.

	Total (n = 281)	Second-generation DSCT (n = 118, 42%) Siemens SOMATOM Definition Flash	Third-generation DSCT (n = 163, 58%) Siemens SOMATOM Force
Muscle	0.90 (0.69–2.35)	2.48 (2.13–2.89)	0.73 (0.61–0.84)
Red bone marrow	0.65 (0.50–1.52)	1.57 (1.35–1.81)	0.52 (0.44–0.59)
Skeleton	2.19 (1.61–5.68)	6.01 (5.14–6.86)	1.67 (1.42–1.98)
Skin	1.14 (0.83–3.05)	3.15 (2.71–3.66)	0.89 (0.75–1.05)
Head and neck			
Brain	1.25 (0.85–2.72)	2.84 (2.30–3.33)	0.92 (0.77–1.09)
Eye lenses	1.72 (1.19–3.89)	4.09 (3.33–4.89)	1.30 (1.06–1.53)
Salivary glands	1.25 (0.85–2.72)	2.84 (2.30–3.33)	0.92 (0.77–1.09)
Thyroid	1.57 (1.14–3.66)	3.92 (3.12–4.79)	1.18 (0.97–1.46)
Chest			
Heart	0.72 (0.57–1.73)	1.77 (1.61–2.04)	0.58 (0.51–0.66)
Lungs	0.82 (0.65–1.98)	2.05 (1.84–2.36)	0.68 (0.58–0.76)
Thymus	0.87 (0.66–2.08)	2.12 (1.91–2.46)	0.69 (0.60–0.80)
Gastrointestinal tract			
Esophagus	0.55 (0.43–1.30)	1.35 (1.20–1.55)	0.44 (0.38–0.51)
Stomach	0.72 (0.57–1.74)	1.79 (1.61–2.07)	0.59 (0.51–0.67)
Small intestine	0.59 (0.47–1.44)	1.48 (1.33–1.70)	0.49 (0.42–0.55)
Colon	0.62 (0.49–1.50)	1.53 (1.37–1.78)	0.51 (0.44–0.58)
Abdominal organs			
Liver	0.72 (0.57–1.73)	1.77 (1.58–2.06)	0.59 (0.51–0.66)
Gallbladder	0.65 (0.51–1.55)	1.61 (1.48–1.85)	0.53 (0.47–0.60)
Pancreas	0.57 (0.46–1.39)	1.42 (1.27–1.64)	0.47 (0.41–0.53)
Spleen	0.70 (0.56–1.68)	1.74 (1.54–2.00)	0.57 (0.49–0.66)
Adrenal glands	0.62 (0.49–1.48)	1.52 (1.37–1.76)	0.51 (0.43–0.58)
Kidneys	0.77 (0.57–1.86)	1.91 (1.71–2.22)	0.63 (0.55–0.72)
Urinary bladder	0.73 (0.57–1.74)	1.79 (1.62–2.06)	0.59 (0.51–0.66)
Reproductive system*			
Testicles	1.83 (1.12–3.56), n = 168	3.58 (2.91–4.11), n = 79	1.14 (0.96–1.32), n = 89
Ovaries	0.50 (0.42–1.28), n = 113	1.45 (1.27–1.72), n = 39	0.45 (0.38–0.50), n = 74
Uterus	0.54 (0.44–1.37), n = 113	1.47 (1.33–1.72), n = 39	0.47 (0.41–0.54), n = 74
Breast	0.85 (0.66–2.01), n = 113	2.24 (1.95–2.99), n = 39	0.72 (0.59–0.85), n = 74

Values are given as median (interquartile range).

*Number of patients for reproductive system organ doses are reported after doses.

DSCT, dual-source computed tomography.

radiographical skeletal survey for the assessment of MM in the range of 0.9–2.5 mSv (6,16–18). Accordingly, effective doses of WBLDCT required about 1.3–3 times the dose of radiographical skeletal surveys (20,27). Our radiation doses undercut the reported data for WBLDCT and were even below several reported doses for radiographic skeletal surveys. Hence, modern CT devices, in particular third-generation DSCT, can achieve low radiation exposure and effective doses. Therefore, an increased radiation burden of WBLDCT is no longer a valid argument to prefer a radiographic skeletal survey when modern CT devices are available. The additional radiation-induced cancer risk of our WBLDCT calculated for a patient with the mean age of the patient cohort (63.8 years) would be 0.22% for second-generation versus 0.13%

for third-generation DSCT (31). Therefore, third-generation DSCT can reduce the radiation burden and radiation-induced cancer risk, which can be important particularly for young patients and those who undergo repeatedly WBLDCT (32,33). Regarding specific organ doses, the highest organ dose was determined at both DSCT generations for the skeleton, where the median effective dose was significantly lower (72%) for third-generation DSCT (1.67 mSv vs 6.01 mSv; $P < 0.001$) (Table 3). According to our results, published dose assessments of WBLDCT for patients with MM reported the highest organ dose for the skeleton, which received an organ dose of 8.4–13.1 mSv (6,17). In the present study, the organ dose for skeleton as well as for other organs were substantially lower, which demonstrates that radiation doses of

WBLDCT can be further reduced with modern DSCT. In addition, all organ doses were significantly lower at third-generation DSCT compared with second-generation DSCT ($P < 0.001$). Several studies reported approaches to reduce radiation doses of WBLDCT by spectral shaping with tin filtration and by iterative reconstruction techniques, which can decrease the median effective dose to 1.45 mSv and provides adequate image quality (16,18,27). Another study assessed spectral shaping by tin filtration at third-generation DSCT and reported an effective dose of 1.0 mSv for WBLDCT (16). However, image quality remains adequate and of diagnostic accuracy. Furthermore, previous studies demonstrated that lowering tube voltage and automated tube modulation reduce radiation doses without lowering image quality (34). Our results show that third-generation DSCT with tin filtration can reduce radiation exposure and effective dose by about 70% compared with second-generation DSCT.

Ionizing radiation exposures of CT techniques vary significantly between different institutions and further due to intrinsic differences of CT devices (35–38). Standardized aggregation of radiation dose data is common practice at our institution as collecting radiation data helps to analyze the dose distribution according to protocol and devices (39). Therefore, DRLs are a helpful benchmark which indicate typical ionizing radiation exposure values for a specific technique (40). Several studies have reported local, regional, or national DRLs for various indications, which is a reasonable solution as equipment and protocols vary by institutions (40). Nonetheless, neither national nor European DRLs are set for WBLDCT. Our radiation exposures and dose estimates were well below the recently published data and show that WBLDCT by third-generation DSCT with modern low-dose techniques can be in line or even undercut the radiation exposure of a radiographic skeletal survey for the assessment of MM. Therefore, our locally determined DRLs may help as benchmarks to revise national and European DRLs and contribute to further radiation protection.

The present study has some limitations. These are the retrospective design and that image quality was not considered when comparing the two different DSCT generations. Thus, all examinations were of diagnostic accuracy as they were acquired and used in clinical routine. Additionally, adequate image quality delivered by WBLDCT with third-generation DSCT has been reported (27). Further, we could not report local radiation doses of the radiographic skeletal survey for MM as we perform WBLDCT for the assessment of MM only. The strengths of the study include the large number of patients assessed by uniform CT protocols

at two different modern DSCTs and the detailed report of radiation exposures and organ doses.

In conclusion, radiation exposure and effective dose of WBLDCT for the assessment of MM were significantly lower by third-generation compared with second-generation DSCT scanners and can even undercut the radiation dose of a typical radiographic skeletal survey. DRLs regarding WBLDCT are required to ensure optimized radiation protection, where our local DRLs may help as benchmarks as they were well below the reported values of recently published dose assessments.

Declaration of conflicting interests

The author(s) declared no potential conflicts of interest with respect to the research, authorship, and/or publication of this article.

Funding

The author(s) received the following financial support for the research, authorship, and/or publication of this article: DB and JH were supported as Clinician Scientists and received research grants within the University Medicine Essen Academy (UMEA) program, funded by the German Research Foundation (DFG; grant FU356/12-1) and the Faculty of Medicine, University of Duisburg-Essen.

ORCID iDs

Sebastian Zensen  <https://orcid.org/0000-0003-2997-0740>
Denise Bos  <https://orcid.org/0000-0002-9585-9787>
Marcel Opitz  <https://orcid.org/0000-0001-7455-8590>
Johannes Haubold  <https://orcid.org/0000-0003-4843-5911>

References

1. Bird JM, Owen RG, D'Sa S, et al. Guidelines for the diagnosis and management of multiple myeloma 2011. *Br J Haematol* 2011;154:32–75.
2. Mahnken AH, Wildberger JE, Gehbauer G, et al. Multidetector CT of the spine in multiple myeloma: comparison with MR imaging and radiography. *AJR Am J Roentgenol* 2002;178:1429–1436.
3. Rajkumar SV, Dimopoulos MA, Palumbo A, et al. International Myeloma Working Group updated criteria for the diagnosis of multiple myeloma. *The Lancet Oncology* 2014;15:e538–e548.
4. Kumar SK, Rajkumar SV, Dispenzieri A, et al. Improved survival in multiple myeloma and the impact of novel therapies. *Blood* 2008;111:2516–2520.
5. Terpos E, Kleber M, Engelhardt M, et al. European Myeloma Network guidelines for the management of multiple myeloma-related complications. *Haematologica* 2015;100:1254–1266.
6. Hemke R, Yang K, Husseini J, et al. Organ dose and total effective dose of whole-body CT in multiple myeloma patients. *Skeletal Radiol* 2020;49:549–554.
7. Horger M, Claussen CD, Bross-Bach U, et al. Whole-body low-dose multidetector row-CT in the diagnosis of

- multiple myeloma: an alternative to conventional radiography. *Eur J Radiol* 2005;54:289–297.
8. Hur J, Yoon C-S, Ryu YH, et al. Efficacy of multidetector row computed tomography of the spine in patients with multiple myeloma: comparison with magnetic resonance imaging and fluorodeoxyglucose-positron emission tomography. *J Comput Assist Tomogr* 2007;31:342–347.
 9. Deak PD, Smal Y, Kalender WA. Multisection CT protocols: sex- and age-specific conversion factors used to determine effective dose from dose-length product. *Radiology* 2010;257:158–166.
 10. Shrimpton PC, Wall BF. The increasing importance of X ray computed tomography as a source of medical exposure. *Radiation Protection Dosimetry* 1995;57:413–415.
 11. European Commission. European guidelines on quality criteria for computed tomography. Report EUR 16262. Luxembourg: Publications Office of the European Union, 1999.
 12. National Council on Radiation Protection and Measurements. Report No. 172 – Reference levels and achievable doses in medical and dental imaging: recommendations for the United States. Bethesda, MD: NCRP, 2012.
 13. Cook TS, Zimmerman S, Maidment ADA, et al. Automated extraction of radiation dose information for CT examinations. *J Am Coll Radiol* 2010;7:871–877.
 14. Fisher DR, Fahey FH. Appropriate use of effective dose in radiation protection and risk assessment. *Health Phys* 2017;113:102–109.
 15. The 2007 Recommendations of the International Commission on Radiological Protection. ICRP publication 103. *Ann ICRP* 2007;37:1–332.
 16. Boyd C, Hickson K. Radiation dosimetry considerations for skeletal survey imaging of multiple myeloma. *Phys Med* 2019;64:109–113.
 17. Kröpil P, Fenk R, Fritz LB, et al. Comparison of whole-body 64-slice multidetector computed tomography and conventional radiography in staging of multiple myeloma. *Eur Radiol* 2008;18:51–58.
 18. Lambert L, Ourednicek P, Meckova Z, et al. Whole-body low-dose computed tomography in multiple myeloma staging: Superior diagnostic performance in the detection of bone lesions, vertebral compression fractures, rib fractures and extraskelatal findings compared to radiography with similar radiation exposure. *Oncol Lett* 2017;13:2490–2494.
 19. Kosmala A, Weng AM, Heidemeier A, et al. Multiple myeloma and dual-energy CT: diagnostic accuracy of virtual noncalcium technique for detection of bone marrow infiltration of the spine and pelvis. *Radiology* 2018;286:205–213.
 20. Dimopoulos M, Terpos E, Comenzo RL, et al. International myeloma working group consensus statement and guidelines regarding the current role of imaging techniques in the diagnosis and monitoring of multiple Myeloma. *Leukemia* 2009;23:1545–1556.
 21. Regelink JC, Minnema MC, Terpos E, et al. Comparison of modern and conventional imaging techniques in establishing multiple myeloma-related bone disease: a systematic review. *Br J Haematol* 2013;162:50–61.
 22. Hillengass J, Fechtner K, Weber MA, et al. Prognostic significance of focal lesions in whole-body magnetic resonance imaging in patients with asymptomatic multiple myeloma. *J Clin Oncol* 2010;28:1606–1610.
 23. Merz M, Hielscher T, Wagner B, et al. Predictive value of longitudinal whole-body magnetic resonance imaging in patients with smoldering multiple myeloma. *Leukemia* 2014;28:1902–1908.
 24. Dimopoulos MA, Facon T, Terpos E, editors. Multiple Myeloma and Other Plasma Cell Neoplasms. Hematologic Malignancies. Cham: Springer International Publishing, 2018.
 25. Amis ES, Butler PF, Applegate KE, et al. American College of Radiology white paper on radiation dose in medicine. *J Am Coll Radiol* 2007;4:272–284.
 26. Brenner DJ, Hall EJ. Computed tomography — an increasing source of radiation exposure. *N Engl J Med* 2007;357:2277–2284.
 27. Suntharalingam S, Mikat C, Wetter A, et al. Whole-body ultra-low dose CT using spectral shaping for detection of osteolytic lesion in multiple myeloma. *Eur Radiol* 2018;28:2273–2280.
 28. Ippolito D, Talei Franzesi C, Spiga S, et al. Diagnostic value of whole-body ultra-low dose computed tomography in comparison with spinal magnetic resonance imaging in the assessment of disease in multiple myeloma. *Br J Haematol* 2017;177:395–403.
 29. Pianko MJ, Terpos E, Roodman GD, et al. Whole-body low-dose computed tomography and advanced imaging techniques for multiple myeloma bone disease. *Clin Cancer Res* 2014;20:5888–5897.
 30. Borggrefe J, Giravent S, Campbell G, et al. Association of osteolytic lesions, bone mineral loss and trabecular sclerosis with prevalent vertebral fractures in patients with multiple myeloma. *Eur J Radiol* 2015;84:2269–2274.
 31. Wall BF, Haylock R, Jansen JTM, et al. Radiation Risks from Medical X-ray Examinations as a Function of the Age and Sex of the Patient. Didcot: Health Protection Agency, 2011.
 32. Marcus RP, Koerner E, Aydin RC, et al. The evolution of radiation dose over time: measurement of a patient cohort undergoing whole-body examinations on three computer tomography generations. *Eur J Radiol* 2017;86:63–69.
 33. Pearce MS, Salotti JA, Little MP, et al. Radiation exposure from CT scans in childhood and subsequent risk of leukaemia and brain tumours: a retrospective cohort study. *Lancet* 2012;380:499–505.
 34. Scholtz J-E, Wichmann JL, Hüsters K, et al. Automated tube voltage adaptation in combination with advanced modeled iterative reconstruction in thoracoabdominal third-generation 192-slice dual-source computed tomography: effects on image quality and radiation dose. *Acad Radiol* 2015;22:1081–1087.
 35. Kalender WA. Computed Tomography: Influence of Exposure Parameters and the Establishment of

- Reference Dose Values. *Radiation Protection Dosimetry* 1998;80:163–166.
36. Smith A, Shah GA, Kron T. Variation of patient dose in head CT. *Br J Radiol* 1998;71:1296–1301.
 37. Smith-Bindman R, Lipson J, Marcus R, et al. Radiation dose associated with common computed tomography examinations and the associated lifetime attributable risk of cancer. *Arch Intern Med* 2009;169:2078–2086.
 38. Héliou R, Normandeau L, Beaudoin G. Towards dose reduction in CT: patient radiation dose assessment for CT examinations at university health center in Canada and comparison with national diagnostic reference levels. *Radiation Protection Dosimetry* 2012;148:202–210.
 39. MacGregor K, Li I, Dowdell T, et al. Identifying Institutional Diagnostic Reference Levels for CT with Radiation Dose Index Monitoring Software. *Radiology* 2015;276:507–517.
 40. Vassileva J, Rehani M. Diagnostic reference levels. *AJR Am J Roentgenol* 2015;204:W1–3.

DuEPublico

Duisburg-Essen Publications online

UNIVERSITÄT
DUISBURG
ESSEN

Offen im Denken

ub | universitäts
bibliothek

This text is made available via DuEPublico, the institutional repository of the University of Duisburg-Essen. This version may eventually differ from another version distributed by a commercial publisher.

DOI: 10.1177/02841851211003287

URN: urn:nbn:de:hbz:465-20220818-113613-0

This publication is with permission of the rights owner freely accessible due to an Alliance licence and a national licence (funded by the DFG, German Research Foundation) respectively.

All rights reserved.